Chemistry Africa
https://doi.org/10.1007/s42250-024-01060-8

ORIGINAL ARTICLE

Advancing Rapid Arsenic (III) Detection Through Device-Integrated Colorimetry

Sumalatha Bonthula[1] · Surya Devarajan[1] · Muni Raj Maurya[1] · Somaya Al-Maadeed[2] · Ramzi Maalej[3] · Mohamed Zied Chaari[4] · Kishor Kumar Sadasivuni[1,5]

Received: 4 January 2024 / Accepted: 14 August 2024

Abstract
It is essential to detect precise traces of inorganic arsenic ions when utilized, which may increase the risks of several health issues such as lung, bladder, skin cancer, and diabetes diseases. In this study, bromocresol green, chlorophenol red, and cresol red dyes were examined to detect the presence of arsenic (III). Further, we present a colorimetric arsenic (III) detection using a cost-effective paper-based sensor and portable device method. The calibration plot from UV-Vis absorption exhibited a detection limit of ~0.054 µM of arsenic (III) in the detection range of 0–10 mM. The selectivity study establishes this method for visual on-site detection of arsenic (III) combined with the simultaneous presence of common coexisting ions. The paper and device-based dual strategy to detect arsenic (III) offered high sensitivity and selectivity under room conditions. Both the paper sensor and the proposed device have a potential for rapid on-site detection of arsenic (III). Therefore, it could provide a viable solution for the design of affordable, sensitive, and portable tools for the environmental monitoring of arsenic (III).

Keywords Arsenic (III) · Dyes · Colorimetry · Paper sensors · Device

1 Introduction

Arsenic, being on the list of Environmental Protection Agency's extremely hazardous substances [1], always plays a major role in environmental pollution due to its functioning towards enzymes, it can change the functioning of around 200 enzymes [2]. Arsenic is widely disseminated in nature, with arsenite (III) and arsenate (V) being the primary inorganic compounds, the trivalent state typically exhibits greater toxicity among all the pertinent inorganic states. Over time, these environmental pollutants accumulate in the soil and groundwater and enter the food chain and into living organisms and plants, which leads to health hazards [3]. As per guidelines established by the World Health Organization, the presence of arsenic in natural and drinking water must be reduced until the concentration falls below 10 parts per billion (ppb) or 0.14 micromoles (µM) [4]. Poultry farming is a significant component of the global food industry, providing a major source of animal protein for human consumption [5]. Poultry can ingest arsenite through contaminated feed, water, and soil. In addition, arsenic-containing drugs are frequently used in poultry as part of their feed, aiming to expedite weight gain [6]. Arsenic-based drugs (roxarsone and nitarsone) have been used in poultry production for decades, which eventually corresponds to an easy source of exposure to arsenic [7, 8]. Chronic exposure to arsenic can lead to reduced growth rates, decreased feed efficiency, and impaired immune function in poultry [9, 10]. This can increase susceptibility to diseases and infections, leading to higher bird mortality rates. The accumulation of arsenic in poultry tissues can lead to its presence in poultry products such as meat and eggs [11–13]. This poses a potential risk to human health, as arsenic-contaminated poultry

✉ Kishor Kumar Sadasivuni
kishorkumars@qu.edu.qa

1 Center for Advanced Materials, Qatar University, PO Box 2713, Doha, Qatar

2 Department of Computer Science and Engineering, Qatar University, PO Box 2713, Doha, Qatar

3 Faculty of Sciences of Sfax, University of Sfax, Sfax, Tunisia

4 Office of Research, Experiments and Development, Ministry of Defense, Doha, Qatar

5 Department of Mechanical and Industrial Engineering, Qatar University, PO Box 2713, Doha, Qatar

Published online: 29 August 2024

products can lead to the transfer of arsenic compounds to humans. Chronic exposure to low levels of arsenic in food has been associated with various health issues in humans, including an increased risk of certain cancers, cardiovascular diseases, and developmental disorders [14, 15]. In a study, arsenic treatment of microglial BV-2 cells results in a dose-dependent reaction. Increased levels of arsenic led to neurotoxic effects [16]. Due to its greater absorption in the gastrointestinal system of a living organism, inorganic arsenic is more hazardous than organic arsenic. In addition to its effects on poultry health and human food safety, arsenic use in poultry farming can also contribute to environmental contamination. Arsenic-containing poultry waste, such as litter and manure, can leach into soil and water systems, leading to soil and water contamination [7]. This can impact aquatic ecosystems and potentially harm other animals and plants. The effects of arsenic on poultry are a growing concern for both poultry farmers and consumers. Arsenic exposure can lead to adverse health effects in poultry, residues in poultry products, and environmental contamination. To mitigate these issues, the poultry industry must adopt frequent and rapid monitoring of the arsenic concentration in the water and feed used in the poultry.

Several instrumental techniques for detecting arsenic include cathodic/anodic stripping voltammetry, plasma mass spectrometry, atomic fluorescence spectrometry and atomic absorption spectrometry [17]. Despite their capability for detecting low levels of arsenic, these methods have drawbacks such as limited onsite functionality, high costs, and the need for highly skilled professionals, which restricts their practical applications. The other analytical detection methods include surface sensing [18–19], colorimetric sensing [17], fluorescence sensing [20] and electrochemical sensing [21–23] etc. These arsenic detection methods show good sensitivity. However, colorimetric-based sensing has the edge over other methods of on-site point-of-use, rapid detection, and visual detection, which establish its applicability in field analysis. Colorimetric sensors are the easiest, most practical, and instrument-free technique [24–27]. An alternative technology for making cost-effective, disposable, portable analytical techniques [28] is paper-based sensors that can be applied in different applications, including environmental, food quality control, clinical diagnosis, etc. Compatibility with chemicals, passive liquid transfer, and biochemicals are the key benefits of utilizing paper as a sensing platform that responds to a quick color shift [29].

Cellulose fibers, the fundamental component of paper, pass a liquid through its hydrophilic fiber matrix [30] and paper-based sensors are highly sensitive for detection. Different compounds, such as nanoparticles, biomolecules (nucleic acids, aptamers, antibodies), and chemo-responsive dyes, can be used to functionalize the paper sensor's surface [31–33]. Due to its key features, including porosity, particle retention, and flow rate, the Whatman cellulose range is frequently employed [34, 35].

The current research proposes a low-cost colorimetric detection for the dynamic identification of arsenic (III). The study aims to identify the arsenic (III) by the dye system, and the proposed method is validated by a dual-strategy using a paper-based sensor and a 3D-printed portable device that can successfully detect and quantify arsenic (III) for real-time rapid on-site applications.

2 Methodology

2.1 Chemicals and Equipment

Sodium arsenite was procured from Research-Lab Fine Chem Industries, Mumbai, India. The dyes Cresol red (CR), chlorophenol red (CPR), and bromocresol green (BCG) were obtained from Sigma Aldrich. The experiments were conducted utilizing Millipore Milli-Q double-distilled water. Characterization was performed using a UV-Vis spectrophotometer (Biochrom Ltd.) capable of scanning within the range of 300 to 800 nm.

2.2 Methods

Figure 1 shows the schematic of the adopted methodology, which involves the preparation of the pH-adjusted dye solutions and analysis of the arsenic (III) detection. Examining the detection sensitivity of the dye by varying the arsenic (III) concentration and analysing with UV-Vis spectroscopy. Real-time on-site applicability proof is established by fabricating a paper-based sensor to detect arsenic (III) visually. Further, we report a 3D-printed and IoT-interfaced prototype for rapid detection and quantification of arsenic (III) based on RGB color space analysis. Adopted methodologies are briefly discussed in the next section.

2.2.1 Preparation of Reagents and Analysis

The experiment used 3 mM BCG, CPR and CR dye solutions for analysis. The pH effect on dye was examined in acidic (3, 5), neutral, and basic (9, 12) solution. Arsenic (III) different molar concentration solution was prepared by dissolving sodium arsenite in DI water. The dyes solution of 10 ml was adjusted to their respective acidic, neutral, and basic mediums pH values and was treated with 1 mL of 10 mM arsenic (III) solution. These test solutions' temperature and concentration effects in dyes were investigated using color change in visible regions at detected pH. The detection limits for the various dyes are investigated using 0–10

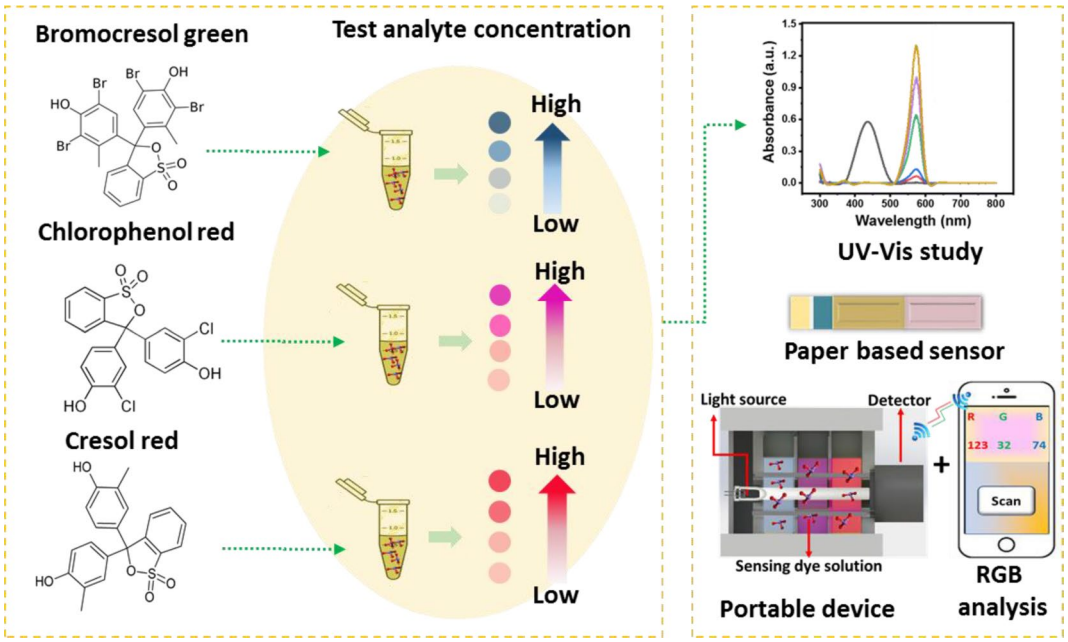

Fig. 1 Schematic representing the adopted methodology

mM concentrations of arsenic (III) solution. The temperature effect was studied at 25–75 °C and 90 °C. With 10 mM arsenic (III), selectivity experiments were performed with respect to different interfering metal ions.

2.2.2 Functionalization for Arsenic (III) Detection

Regarding cost, affordability, and access to functionalization techniques, employing paper as a platform for sensing devices is more advantageous. Since the paper device may be activated using very little chemical input, it is extremely cost-effective. Whatman No. 1 filter paper is an appropriate tool due to its hydrophilic properties and porous structure, which helps in its fast adsorption of dye solutions. To functionalize the paper sensor, Whatman paper was soaked for one hour in pH 3 adjusted 3 mM BCG, CPR and CR dye solution and dried overnight at room temperature. For further analysis, the dye-absorbed filter paper was cut into strips.

2.2.3 3D-printed and smartphone-interfaced Sensor Prototype

We developed a 3D-printed colorimetric device with open-source hardware and software. The design of the colorimeter involved breaking down the assembly into three distinct parts: the light source section, the sample area, and the color detection region. In the light source section, we incorporated the white light LED. The sample area followed the light source. Each chamber held a cuvette containing a separate dye solution, stacked vertically and sequentially. To safeguard the sample area, a protective 3D-printed case was employed. The color detector area was adjacent to the sample area, consisting of RBG analysing photodetector. The process commenced with light emanating from the LED source and passing through the dye solutions' cuvettes. Subsequently, the photodetector captured the RGB value of the transmitted light from the sample area. When exposed to arsenic (III), the dye solutions changed color. These changes were identified by the detector, resulting in distinctive RGB values. These values were then displayed on a connected device (such as an LCD or smartphone) linked to the sensor prototype via Bluetooth.

3 Results and Discussion

3.1 pH Effect

The pH effect for detecting 10 mM arsenic (III) at room temperature was investigated with dye solutions in acidic, basic, and neutral mediums. The solutions were examined before and after adding test analyte in various pH adjusted dyes solutions. Within a few seconds, all dyes could produce noticeable color changes. After adding 10 mM arsenic (III), the BCG dye color in an acidic medium (pH 3), changed from yellow to light blue. A clear color change is observed for pH 3 after adding 10 mM arsenic (III), as shown in Fig. 2a. From Fig. 2b, the color change was confirmed by the emergence of a new absorption band centered at 618 nm and extinction of band at 448 nm in UV-Vis absorbance

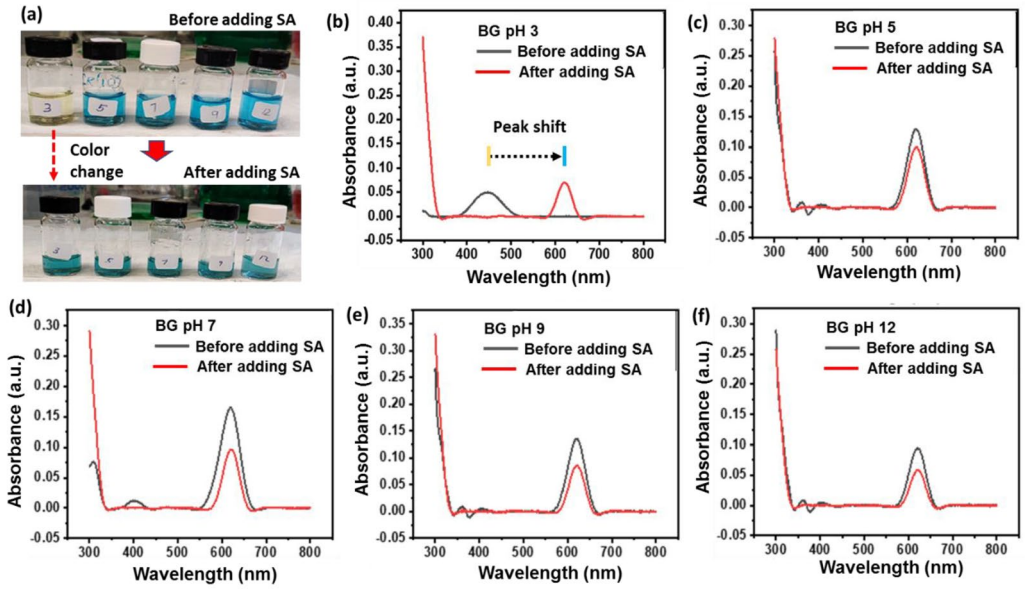

Fig. 2 Detection of arsenic (III) by bromocresol green dye solution (BCG). (**a**) BCG dye solution before and after adding the 10 mM arsenic (III) solution. (**b-f**) Absorbance spectra of bare BCG dye solution and after adding 10 mM arsenic (III) in acidic (pH 3, pH 5), neutral (pH 7) and basic medium (pH 9, pH 12), respectively

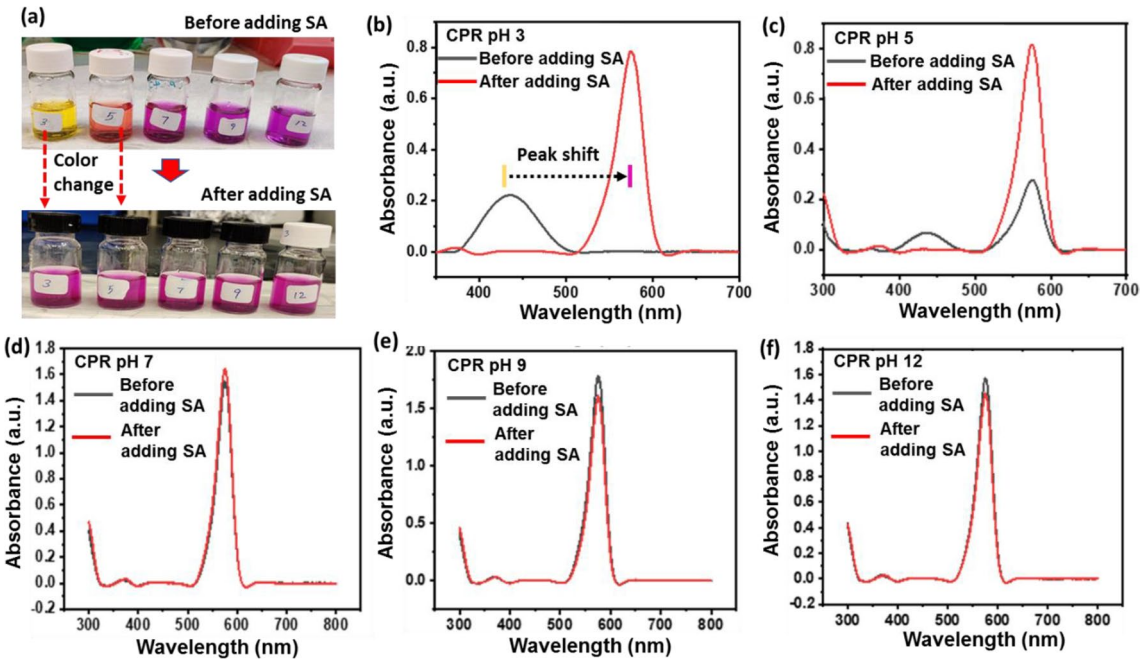

Fig. 3 Detection of arsenic (III) by chlorophenol red (CPR) dye. (**a**) CPR dye solution before and after the addition of the 10 mM arsenic (III) solution. (**b-f**) UV-Vis absorbance spectra of bare CPR dye solution and after adding 10 mM arsenic (III) in acidic (pH 3, pH 5), neutral (pH 7) and basic medium (pH 9, pH 12), respectively

spectra. Figure 2c-f shows the UV-Vis absorption spectra of pH 5, pH 7, pH 9 and 12 adjusted BCG dye solution before and after adding the 10 mM arsenic (III), respectively.

During analysis 10 mM arsenic (III) was added pH adjusted solutions of chlorophenol red, and a noticeable color change was evident in pH 3 and pH 5 solutions. In pH 3 and pH 5 dye solutions, the color changed from yellow to magenta and orange to magenta, respectively, as shown in Fig. 3a. The UV-Vis absorbance spectra displayed the emergence of a new absorption band centered at ~ 575 nm for pH 3 dye solutions, as shown in Fig. 3b. The peak at 437 nm disappeared, and a new peak at 575 nm appeared with very

high intensity for pH 3, indicating a visible color change of the dye solution after adding 10 mM arsenic (III). While, for pH 5 dye solution, the bare and 10 mM arsenic (III) added dye solution both exhibited a peak at ~575 nm, and the peak at 437 nm disappeared after adding arsenic (III), as shown in Fig. 3c. In contrast, no visible color change was noticed for pH 7, pH 9 and pH 12 dye solution after adding 10 mM arsenic (III), absorbance spectra confirmed the same with no peak shift, as shown in Fig. 3d-f, respectively.

Similarly, an apparent color change was observed by adding 10 mM arsenic (III) to pH-adjusted solutions of cresol red. The color shifted from yellow to magenta in pH 3, pH 5, and pH 7. In contrast, in pH 9, the color changed from red to magenta, as shown in Fig. 4a. From the absorbance spectra, a new absorption band positioned at 573 nm for pH 3, pH 5 and pH 7 dye solutions was observed that corresponded to the color change after the addition of arsenic (III), as shown in Fig. 4b-d, respectively. For the pH 9 dye solution, the peak at 436 nm disappeared, and the intensity of the peak at 574 nm was enhanced, as shown in Fig. 4e. While for pH 12, no peak shift was noticed in the absorbance spectra after adding 10 mM arsenic (III), as shown in Fig. 4f.

3.2 Effect of the Concentration

By adjusting the arsenic (III) concentration from 0 to 10 mM, the reactive pH 3 adjusted solution at room temperature was used to evaluate the dyes' sensitivity towards the arsenic (III) detection. Further UV spectrophotometric analysis was performed to estimate the limit of detection (LOD) of the dyes. Figure 5a, 5c and 5e represent the absorbance plot of BCG, CPR and CR dye solutions after adding 0–10 mM arsenic (III) solution, respectively. The dye solutions successfully produced a visible color shift in the 0–10 mM of arsenic (III) solution. Five samples were analyzed for each arsenic (III) concentration to produce the calibration plot for estimating the BCG, CPR and CR dye LOD for arsenic (III) sensing, as shown in Fig. 5b, 5d and 5f, respectively. The peak absorbance of each dye at various concentrations of specific test analytes was employed to create the calibration curve. The BCG had an absorbance peak at 618 nm, CPR at 575 nm, and CR at 573 nm, as shown in Fig. 5a, 5c and 5e, respectively.

Using Eq. 1, the LOD is determined by the linear fitting of the graph in the detection range of 0–10 mM of arsenic (III) solution.

$$\mathrm{LOD} = \frac{3\sigma}{\mathrm{m}} \tag{1}$$

where m is the slope of the calibration plots, and σ is the standard deviation of the intercept. The estimated LOD of the linear fitting of BCG is 0.2 µM, $R^2 = 0.98$. In CPR, the calculated LOD for various arsenic (III) concentrations ranging from 0 to 10 mM was 0.054 µM with $R^2 = 0.99$. Similarly, the LOD of CR was 0.3 µM with $R^2 = 0.99$. Further, CPR dye exhibited the lowest linear detection limit, i.e. 0.054 µM in the concentration range of 0–10 mM. The

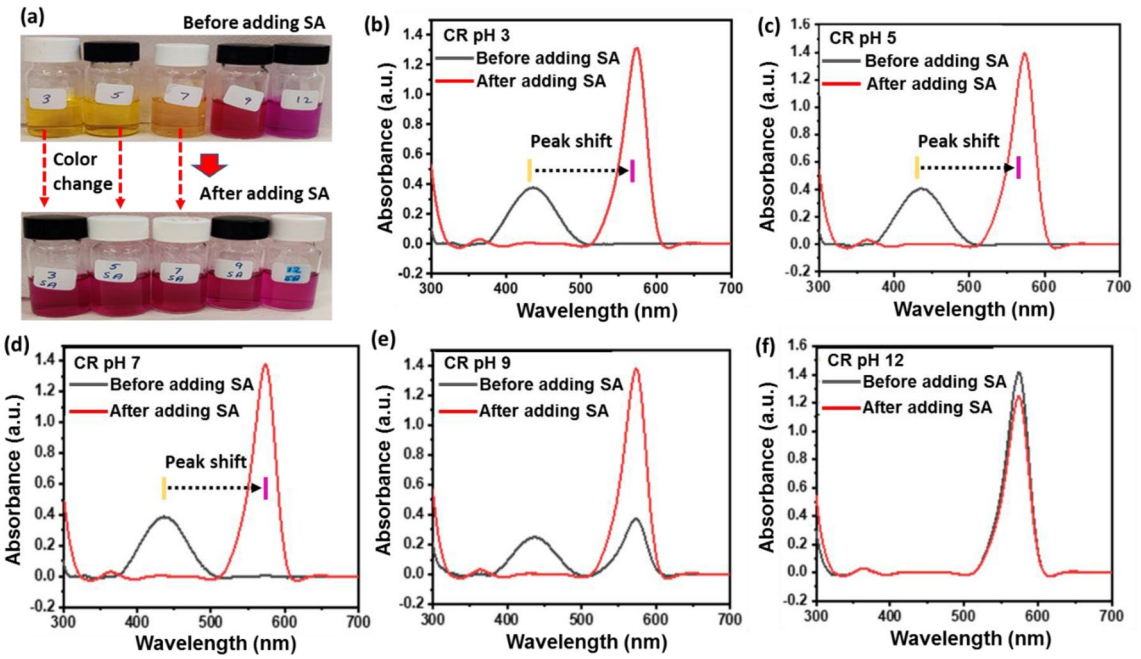

Fig. 4 Detection of arsenic (III) by cresol red (CR) dye. (**a**) CR dye solution before and after adding the 10 mM arsenic (III) solution. (**b-f**) UV-Vis absorbance spectra of bare CR dye solution and after adding 10 mM arsenic (III) in acidic (pH 3, pH 5), neutral (pH 7) and basic medium (pH 9, pH 12), respectively

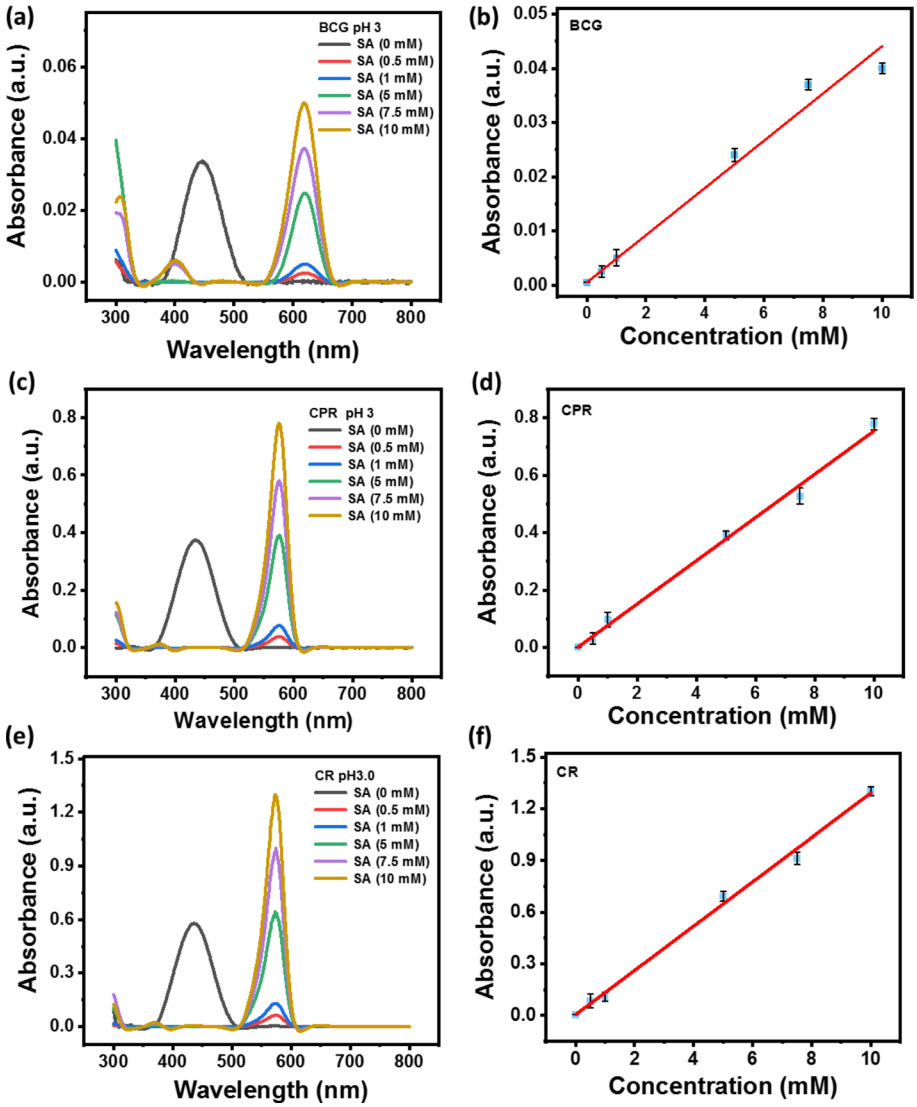

Fig. 5 Dyes sensitivity towards arsenic (III) sensing. (**a**, **c**, **e**) UV-Vis absorption plot of BCG, CPR and CR dye with change in arsenic (III) concentration from 0–10 mM, respectively. (**b**, **d**, **f**) Calibration plot of BCG dye, CPR dye, and CR dyes, respectively

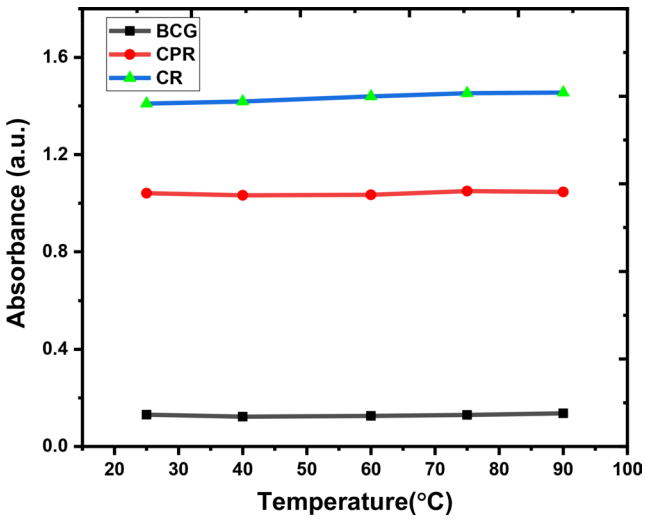

Fig. 6 Temperature effect of 10 mM arsenic (III) in cresol red, chlorophenol red and bromocresol green, dye solutions

sensitivity analysis establishes that all three dyes have a high sensitivity towards arsenic (III) detection.

3.3 Effect of Temperature

An essential feature of the sensor is maintaining its response stability with changes in temperature. Thus, to examine the constancy of the dye response, the dye solution was exposed to different temperatures in the 25–100 °C range. For all dye solutions, 1 mL of the test solution with a concentration of 10 mM arsenic (III) at different temperatures was analyzed, and UV-Vis spectra were obtained. From the absorbance spectra, it was observed that the peak absorption intensity remained almost constant for all dyes, irrespective of the change in the temperature (see Fig. 6). Also, it is noticeable that there is no significant deviation of the absorbance at different temperatures during the stability analysis, indicating

good stability of the dye sensing solution with temperature change.

3.4 Selectivity Study

The selectivity of dyes to arsenic (III) was studied by interferences assessment exposing dye solutions to salts of Cl^{1-}, Ce^{4+}, Co^{2+}, Pb^{2+}, and Cr^{3+}, at a concentration of 10 mM.

The confirmation of selectivity involved assessing the relative change in wavelength ($\Delta\lambda$) using UV-Vis analysis, which was determined using Eq. 2

$$\Delta\lambda = \frac{(\lambda_x - \lambda_o)}{\lambda_o} \times 100 \quad (2)$$

Where λ_x signifies the wavelength at which maximum absorption occurs in the presence of the analyte (BCG $\lambda_x = 618$ nm, CPR $\lambda_x = 575$ nm, CR $\lambda_x = 573$ nm), and λ_o corresponds to the wavelength of peak absorbance of bare dye solution. For all dye solutions, the value is measured to be at pH 3. The BCG, CPR and CR dye solutions exhibited high selectivity and responded only to the test solutions containing arsenic (III), as shown in Fig. 7a (left), 7b (left) and 7c (left), respectively. Based on the data, it can be observed that all dye solutions exhibited significant high selectivity for arsenic (III) with respect to the other interfering species. The binding of the arsenic (III) with BCG, CPR and CR dye results in formation of complex structure that causes a shift in the absorption spectrum, leading to a visible color change. At pH 3 the electrostatic attraction of arsenic with dyes and protonated As-O-H bond formation results in more stable complex formation compared to other interfering species. As a result, the dyes exhibit high selectivity towards arsenic (III). The corresponding chemical reaction of the arsenic (III) with BCG, CPR and CR is presented in Fig. 7a (right), 7b (right) and 7c (right), respectively. The results establish this method for visual on-site detection of arsenic (III) combined with simultaneous presence of common coexisting ions. Table 1 compares the outcomes of this

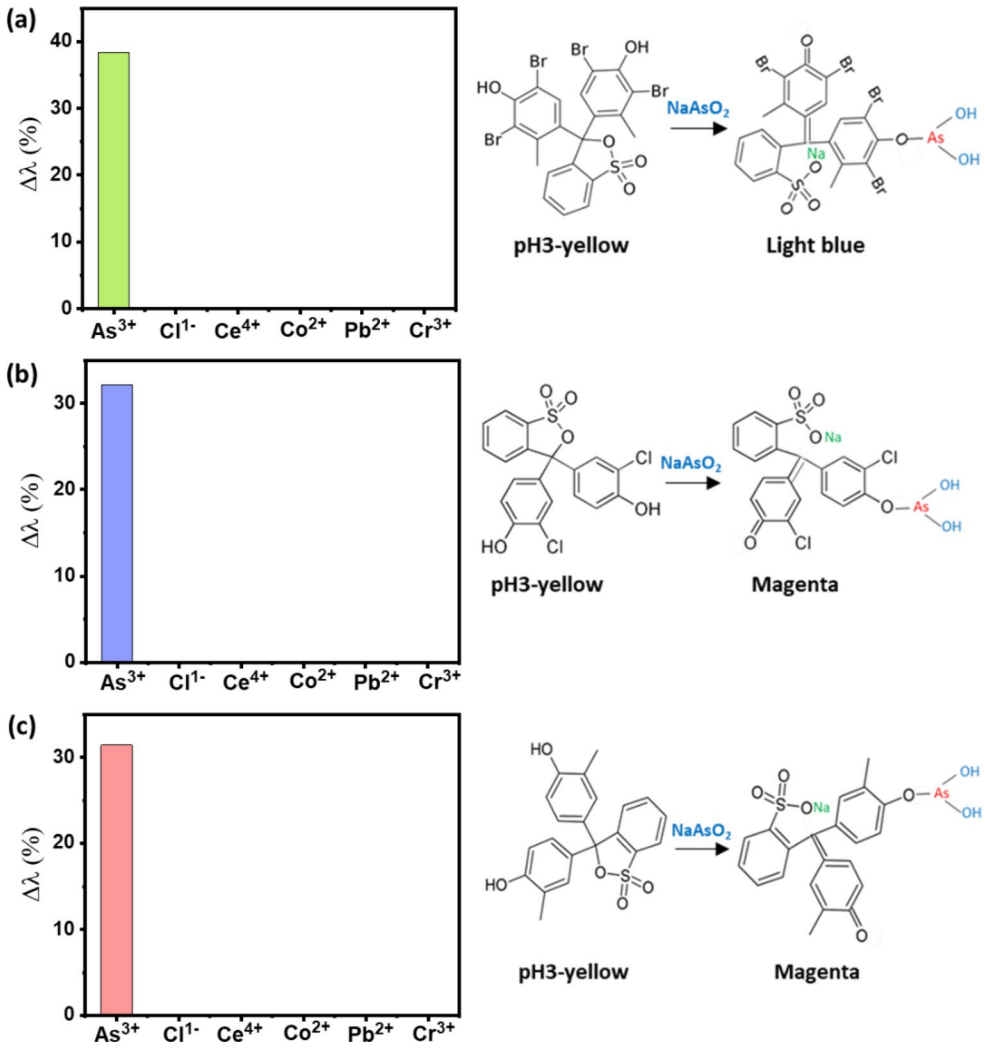

Fig. 7 Selectivity analysis of dyes for 10 mM As^{3+}, Cl^{1-}, Ce^{4+}, Co^{2+}, Pb^{2+} and Cr^{3+} concentrations and possible complex formation of dyes with arsenic (III). (**a**) Bromocresol green. (**b**) Chlorophenol red (**c**) Cresol red dye solutions

Table 1 Comparison of analytical parameters of the proposed colorimetric sensor with other reported sensors

Method	Detection Nature	Linear range	LOD	Reference
PAT-AM-AA	Colorimetric (visual)	0–250 μg L^{-1}	10 μg L^{-1}	[17]
Au-CD	SPR	0.025–0.75 μg L^{-1}	0.01 μg L^{-1}	[18]
CTAB-AuNPs	SPR	1.0-100 ppb	16.9 ppb	[19]
Acf-RhB	Florescence (digital)	0.04–0.09 mg L^{-1}	10 μg L^{-1}	[20]
AAGO-PDDA-PA	Electrochemical (digital)	Up to 30 μM	8.99 ppb	[21]
AuNPs	Electrochemical (digital)	-	16.73 μg L^{-1}	[22]
BDD-AuNPs	Electrochemical (digital)	0.1 to 1.5 ppm	20 ppb	[23]
Bromocresol green (BCG) Chlorophenol red (CPR Cresol red (CR)	Colorimetric (Visual) (RGB analysis)	0–10 mM	BCG- 15 μg L^{-1} CPR- 4 μg L^{-1} CR-22 μg L^{-1}	**Present work**

PAT-AM-AA: Potassium antimonyl tartrate-ammonium molybdate and ascorbic acid, Au-CD: Au-doped carbon dots, CTAB-AuNPs: cetyltrimethylammonium bromide on gold nanoparticles, Acf-RhB: Acriflavine and Rhodamine B dye, AAGO-PDDA-PA: acrylic acid-modified graphene oxide doped polyaniline and poly (diallyl dimethyl ammonium chloride) composite. AuNPs: gold nanoparticle, NBBSH: (E)-N′-(2-Nitrobenzylidene)- benzenesulfonohydrazide, AuNPs-BDD: Boron-doped diamond electrode decorated with gold nanoparticle. SPR-Surface plasmon resonance

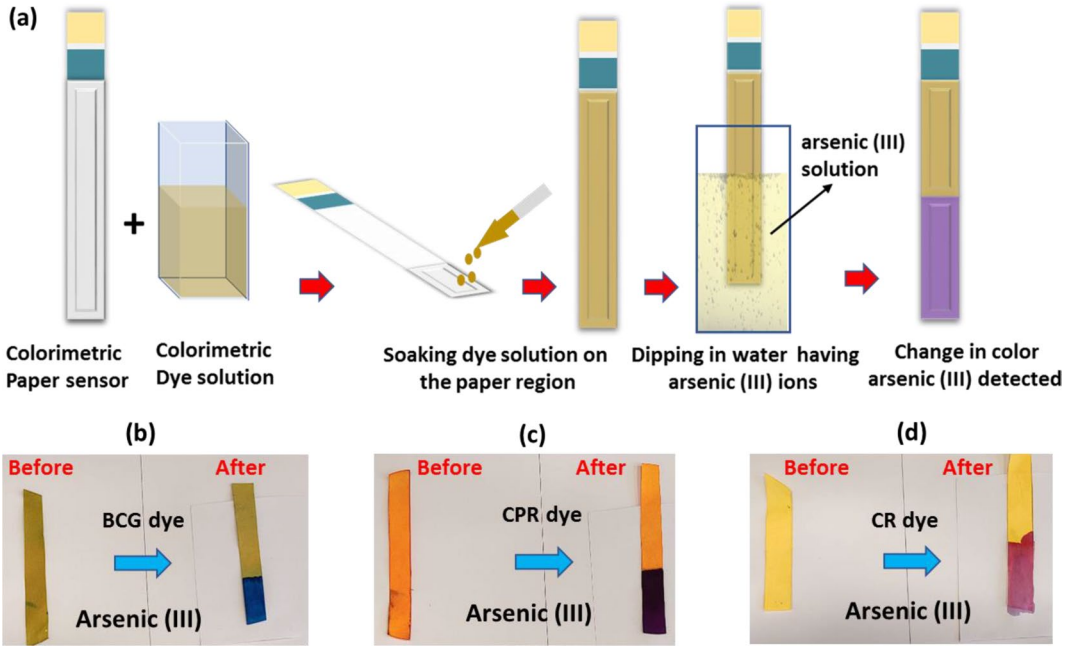

Fig. 8 (**a**) Schematic illustrating the fabrication of colorimetic paper sensor strip and detection of arsenic (III). Real-time assessment for arsenic (III) detection using paper strips modified with (**b**) Bromocresol green dye. (**c**) Chlorophenol red dye. (**d**) Cresol red dye

sensor with prior studies and highlight the significance of the proposed selective sensor.

3.5 Paper-Based Chemo Sensor for Real-Time Detection of Arsenic (III)

To validate the real-time applicability of the proposed method, paper-based sensor was fabricated, and the performance of colorimetric paper sensors was evaluated for detecting 1 mM arsenic (III) in water. Due to the hydrophilic nature and porous structure of the Whatman no.1 paper, fast adsorption of the dye solutions is observed. Hence, it is used as a suitable tool as a sensing device that offers significant advantages with respect to affordability and functionalization processes. Figure 8a shows the schematic for fabricating a colorimetric paper sensor and detecting arsenic (III) ions in water. The filter strips were exposed to arsenic (III) containing water, and color change was observed. The

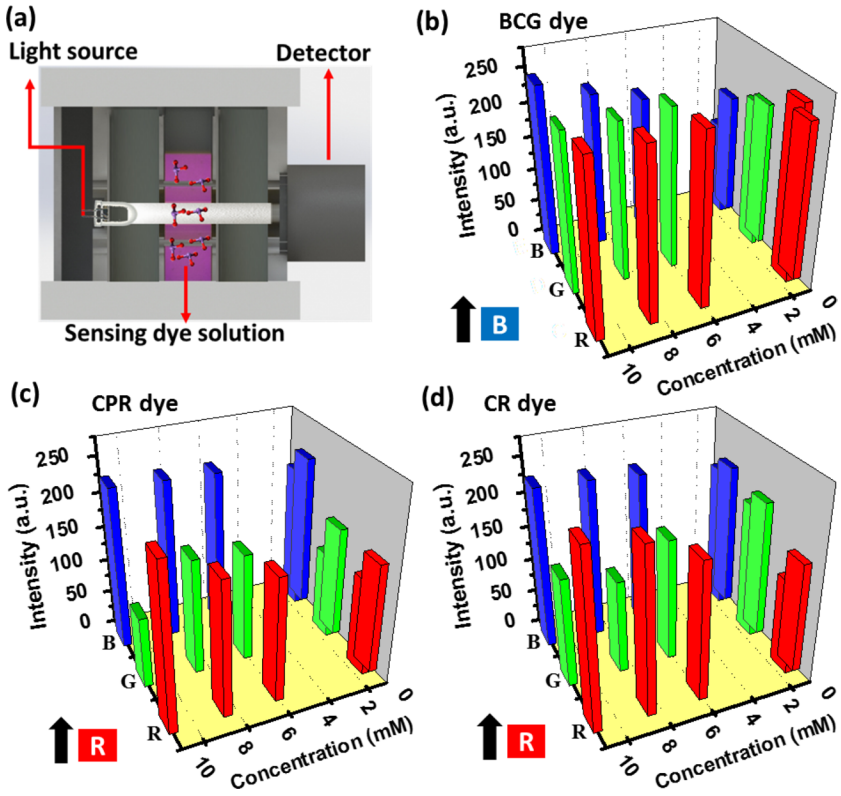

Fig. 9 (**a**) Schematic of the developed 3D-printed sensor device, illustrating colorimetric-based detection of arsenic (III) using RGB analysis. (**b-d**) RGB color space value plot for detecting arsenic (III) using bromocresol green (BCG), chlorophenol red (CPR) and cresol red (CR) dye, respectively

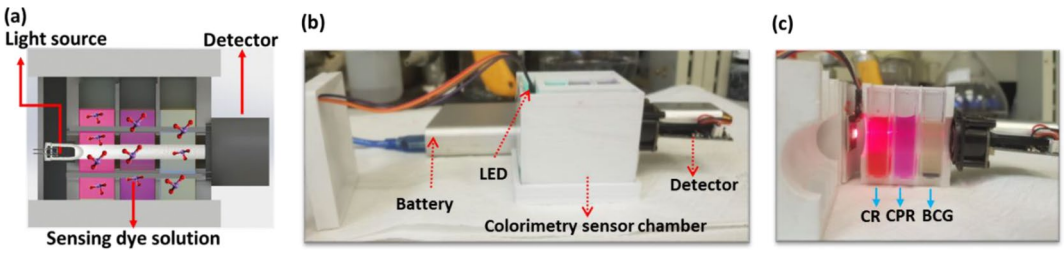

Fig. 10 (**a**) Schematic of the fabricated sensor prototype employing three dye system. (**b**) A picture representing various components embedded in the prototype. (**c**) A real-time picture of the prototype with three dye configurations

sensor strips performed well in detecting arsenic (III). When BCG, CPR and CR dye-soaked paper sensor strips were dipped in water containing arsenic (III) ions, the colour shifted from greenish yellow to blue colour, dark yellow to magenta and yellow to light purple, as shown in Fig. 8b, 8c and 8d respectively.

3.6 Sensor Prototype for Real-Time Detection and Quantification of Arsenic (III)

A functional portable prototype device designed to detect and quantify arsenic (III) was developed, as shown in Fig. 9a. Initially single dye solution was analyzed as sensing elements, and the device exhibited distinctive RGB color space values upon exposure to various concentrations (ranging from 0 to 10 mM) of arsenic (III). Graphs illustrating the RGB color space values corresponding to varying concentrations of arsenic (III) are depicted in Fig. 9b-d. The detection of arsenic (III) using BCG dye displayed an almost linear increase in the 'B' color space value as the concentration of arsenic (III) increased (see Fig. 9b). While, for CPR and CR dye, an increment in arsenic (III) concentration increased the 'R' color space value, as demonstrated in Fig. 9c and 9d, respectively. Thus, by analyzing the 'B' color space value of BCG dye and 'R' color space value in the case of CPR and CR dye, the arsenic (III) concentration can be evaluated.

Further, the developed functional prototype was employed to detect and quantify arsenic (III) by employing three dye system, as shown in Fig. 10a. The developed prototype's different embedded component and real time sensing image is shown in Fig. 10b and 10c, respectively. The three-dye system strategy can provide an accurate and reliable method for the on-site detection of arsenic (III).

Table 2 RGB value chart for 1 mM arsenic (III) in different configuration of dye set

Dye configuration	RGB VALUES
BCG(Nil) CPR(Nil) CP(Nil)	230,210,180
BCG(As(III)) CPR(Nil) CP(Nil)	155,161,223
BCG(Nil) CPR(As(III)) CP(Nil)	158,199,210
BCG(Nil) CPR(Nil) CP(As(III))	165,201,239
BCG(As(III)) CPR(As(III) CP(Nil)	175,118,153
BCG(As(III)) CPR(Nil) CP(As(III)	181,210,194
BCG(Nil) CPR(As(III) CP(As(III))	194,210,176
BCG(As(III)) CPR(As(III) CP(As(III))	210,190,201

Utilizing the three dyes as the sensing components, we can detect arsenic (III) based on the RGB color space chart. The sensor prototype exhibited distinct RGB color space values when a different combination of dyes was exposed to 1 mM arsenic (III), as shown in Table 2. The study demonstrated that we could create a unique RGB color space chart for each concentration of arsenic (III). Each distinct RGB color space value chart correlated to a specific arsenic (III) concentration. This correlation could be utilized to quantify arsenic (III) within the test sample.

4 Conclusion

In this study, a highly sensitive and selective paper sensor and device prototype is developed for the rapid detection of trace level arsenic (III) at ambient temperature. Detection of arsenic (III) was successfully demonstrated by bromocresol green (BCG), chlorophenol red (CPR) and cresol red (CR) dyes. Compared with other dyes, CPR displayed high sensitivity with a visual detection limit of 0.054 µM in the detection range of 0–10 mM. The stability of the dyes was examined with change in the temperature, and all the dyes exhibited high stability towards temperature variation. Further, all three dyes exhibited high selectivity with other interfering molecules. The rapid real-time detection was validated by fabricating paper strips and a 3D-printed device prototype. The paper sensor successfully demonstrated the detection of arsenic (III) through color change within 3 s. The dye-coated paper sensor are cost-effective and can visually detect arsenic (III) just by a change in color, and the response time is 3 s. In addition, the RGB color space value analysis method using the 3D-printed prototype established the detection and quantification of arsenic (III) with a unique RGB color space chart. Both paper- and device-based dual strategies have high stability, and good selectivity. The proposed technology provides a reliable and simple analytical method for environmental monitoring of arsenic (III).

Acknowledgements This work was supported by Qatar National Research Fund under the grant no. MME03-1226-210042. The statements made herein are solely the responsibility of the authors.

Funding This work was supported by Qatar National Research Fund under the grant no. MME03-1226-210042. Open access funding provided by Qatar National Library.
Open Access funding provided by the Qatar National Library.

Data Availability The data supporting the findings of this study are available on request from the corresponding author.

Declarations

Ethical Approval Not applicable.

Informed Consent Not applicable.

Conflict of Interest Not applicable.

References

1. Yadav MK, Saidulu D, Ghosal PS, Mukherjee A, Gupta AK (2022) A review on the management of arsenic-laden spent adsorbent: insights of global practices, process criticality, and sustainable solutions. Environ Technol Innov 27:102500
2. Sodhi KK, Kumar M, Agrawal PK, Singh DK (2019) Perspectives on arsenic toxicity, carcinogenicity and its systemic remediation strategies. Environ Technol Innov 16:100462
3. Jan FA, Ishaq M, Khan S, Ihsanullah I, Ahmad I, Shakirullah M (2010) A comparative study of human health risks via consumption of food crops grown on wastewater irrigated soil (Peshawar) and relatively clean water irrigated soil (lower dir). J Hazard Mater 179(1):612–621
4. Nyangi MJ (2021) Remediation of Arsenic from Water using Iron and Aluminum electrodes in Electrocoagulation Technology: Adsorption Isotherm and Kinetic studies. Chem Afr 4:943–954
5. Connolly G, Clark CM, Campbell RE, Byers AW, Reed JB, Campbell WW (2022) Poultry consumption and Human Health: how much is really known? A systematically searched Scoping Review and Research Perspective. Adv Nutr 13:2115–2124
6. Nigra Anne E, Nachman Keeve E, Love David C, Grau-Perez M, Navas-Acien A (2017) Poultry consumption and Arsenic exposure in the U.S. Population. Environ Health Perspect 125:370–377
7. Yang Z, Peng H, Lu X, Liu Q, Huang R, Hu B, Kachanoski G, Zuidhof MJ, Le XC (2016) Arsenic metabolites, including N-Acetyl-4-hydroxy-m-arsanilic Acid, in Chicken litter from a roxarsone-feeding study involving 1600 chickens. Environ Sci Technol 50:6737–6743
8. Liu Q, Peng H, Lu X, Zuidhof Martin J, Li X-F, Le XC (2016) Arsenic species in Chicken breast: temporal variations of

metabolites, Elimination Kinetics, and residual concentrations. Environ Health Perspect 124:1174–1181
9. Wang Y, Zhao H, Shao Y, Liu J, Li J, Luo L, Xing M (2018) Copper (II) and/or arsenite-induced oxidative stress cascades apoptosis and autophagy in the skeletal muscles of chicken. Chemosphere 206:597–605
10. Wang Y, Zhao H, Guo M, Shao Y, Liu J, Jiang G, Xing M (2018) Arsenite renal apoptotic effects in chickens co-aggravated by oxidative stress and inflammatory response. Metallomics 10:1805–1813
11. ŽIvkov BaloŠ M, JakŠIĆ S, LjubojeviĆ PeliĆ D (2019) The role, importance and toxicity of arsenic in poultry nutrition. Worlds Poult Sci J 75:375–386
12. Ghosh A, Awal MA, Majumder S, Mostofa M, Khair A, Islam MZ, Rao DR (2012) Arsenic in eggs and excreta of laying hens in Bangladesh: a preliminary study. J Health Popul Nutr 30(4):383–393
13. Mondal NK (2020) Prevalence of Arsenic in chicken feed and its contamination pattern in different parts of chicken flesh: a market basket study. Environ Monit Assess 192:590
14. Fatoki JO, Badmus JA (2022) Arsenic as an environmental and human health antagonist: a review of its toxicity and disease initiation. J Hazard Mater Adv 5:100052
15. Muzaffar S, Khan J, Srivastava R, Gorbatyuk MS, Athar M (2023) Mechanistic understanding of the toxic effects of arsenic and warfare arsenicals on human health and environment. Cell Biol Toxicol 39:85–110
16. Kharroubi W, Haj Ahmed S, Nury T, Andreoletti P, Sakly R, Hammami M et al (2017) Mitochondrial dysfunction, oxidative stress and apoptotic induction in microglial BV-2 cells treated with sodium arsenate. J Environ Sci 51:44–51
17. Das J, Sarkar P (2016) A new dipstick colorimetric sensor for detection of arsenate in drinking water. Environ Sci: Water ResTechno 2:693–704
18. Zhang Z-H, Lei K-N, Li C-N, Luo Y-H, Jiang Z-L (2020) A new and facile nanosilver SPR colored method for ultratrace arsenic based on aptamer regulation of Au-doped carbon dot catalytic amplification. Spectrochim Acta Mol Biomol Spectrosc 232:11817
19. Thao Nguyen NL, Park CY, Park JP, Kailasa SK, Park TJ (2018) Synergistic molecular assembly of an aptamer and surfactant on gold nanoparticles for the colorimetric detection of trace levels of As3 + ions in real samples. New J Chem 42:11530–11538
20. Saha J, Roy AD, Dey D, Nath J, Bhattacharjee D, Hussain SA (2017) Development of arsenic(V) sensor based on fluorescence resonance energy transfer. Sens Actuators B Chem 241:1014–1023
21. Hamid Kargari S, Ahour F, Mahmoudian M (2023) An electrochemical sensor for the detection of arsenic using nanocomposite-modified electrode. Sci Rep 13:8816
22. Sullivan C, Lu D, Senecal A, Kurup P (2021) Voltammetric detection of arsenic (III) using gold nanoparticles modified carbon screen printed electrodes: application for facile and rapid analysis in commercial apple juice. Food Chem 352:129327
23. Pungjunun K, Chaiyo S, Jantrahong I, Nantaphol S, Siangproh W, Chailapakul O (2018) Anodic stripping voltammetric determination of total arsenic using a gold nanoparticle-modified boron-doped diamond electrode on a paper-based device. Microchim Acta 185:324
24. Sha MS, Maurya MR, Chowdhury MEH, Muthalif AGA, Al-Maadeed S, Sadasivuni KK (2022) A smartphone-interfaced, low-cost colorimetry biosensor for selective detection of bronchiectasis via an artificial neural network. RSC Adv 12:23946–23955
25. Maurya MR, Onthath H, Morsy H, Riyaz N-USS, Ibrahim M, Ahmed AE et al (2021) Colorimetry-based detection of nitric oxide from exhaled breath for quantification of oxidative stress in human body. Healthcare 9:1055
26. Sha MS, Maurya MR, Geetha M, Kumar B, Abdullah AM, Sadasivuni KK (2022) A Smart Colorimetric Platform for Detection of Methanol, ethanol and formic acid. Sensors 22:618
27. Sha MS, Maurya MR, Shafath S, Cabibihan J-J, Al-Ali A, Malik RA, Sadasivuni KK (2022) Breath analysis for the in Vivo Detection of Diabetic Ketoacidosis. ACS Omega 7:4257–4266
28. Dungchai W, Chailapakul O, Henry CS (2011) A low-cost, simple, and rapid fabrication method for paper-based microfluidics using wax screen-printing. Analyst 136:77–82
29. Xiao-wei H, Xiao-bo Z, Ji-yong S, Zhi-hua L, Jie-wen Z (2018) Colorimetric sensor arrays based on chemo-responsive dyes for food odor visualization. Trends Food Sci Technol 81:90–107
30. Martinez AW, Phillips ST, Whitesides GM, Carrilho E (2010) Diagnostics for the developing world: Microfluidic Paper-based Analytical devices. Anal Chem 82:3–10
31. Li Z, Suslick KS (2018) Ultrasonic Preparation of porous silica-dye microspheres: sensors for quantification of urinary trimethylamine N-Oxide. ACS Appl Mater Interfaces 10:15820–15828
32. Irvine GW, Tan SN, Stillman MJ (2017) A simple metallothionein-based Biosensor for enhanced detection of Arsenic and Mercury. Biosensors 7:1–14
33. Hou XD, Guan XQ, Cao YF, Weng ZM, Hu Q, Liu HB, Hou J (2020) Inhibition of pancreatic lipase by the constituents in St. John's wort: in vitro and in silico investigations. Int J Biol Macromol 145:620–633
34. Songjaroen T, Dungchai W, Chailapakul O, Laiwattanapaisal W (2011) Novel, simple and low-cost alternative method for fabrication of paper-based microfluidics by wax dipping. Talanta 85:2587–2593
35. Geetha M, Kallingal N, Sha MS, Sadasivuni KK, Sawali M, Alsaedi F et al (2022) Versatile inexpensive paper-based chemosensor to detects trimethylamine: a proof of concept. Sens Actuator Phys 338:113437